Cancer Immunology Research 2019; 7 (5): 701-706. DOI: 10.1158/2326-6066.CIR-18-0777

# Responsiveness to PD-1 Blockade in End-Stage Colon Cancer with Gene Locus 9p24.1 Copy-Number Gain

Anne Hansen Ree[1,2], Vigdis Nygaard[3], Hege G. Russnes[4,5], Daniel Heinrich[1], Vegard Nygaard[6], Christin Johansen[1], Inger Riise Bergheim[5], Eivind Hovig[3,7,8,9], Klaus Beiske[4,2], Anne Negård[10,2], Anne-Lise Børresen-Dale[5,2], Kjersti Flatmark[3,11,2,*], and Gunhild M. Mælandsmo[3,12,*]

[1]Department of Oncology, Akershus University Hospital, Lørenskog, Norway. [2]Institute of Clinical Medicine, University of Oslo, Oslo, Norway. [3]Department of Tumor Biology, Oslo University Hospital, Oslo, Norway. [4]Department of Pathology, Oslo University Hospital, Oslo, Norway. [5]Department of Cancer Genetics, Oslo University Hospital, Oslo, Norway. [6]Department of Core Facilities, Oslo University Hospital, Oslo, Norway. [7]Institute for Cancer Genetics and Informatics, Oslo University Hospital, Oslo, Norway. [8]Institute of Computer Science, University of Oslo, Oslo, Norway. [9]Norwegian Cancer Genomics Consortium, Oslo, Norway. [10]Department of Radiology, Akershus University Hospital, Lørenskog, Norway. [11]Department of Gastroenterological Surgery, Oslo University Hospital, Oslo, Norway. [12]Institute for Medical Biology, University of Tromsø–The Arctic University of Norway, Tromsø, Norway. * Equal contributions

**Running Title:** Colon Cancer 9p24.1 Copy-Number Gain and Checkpoint Blockade

**Corresponding Author:** Anne Hansen Ree, Department of Oncology, Akershus University Hospital, P.O. Box 1000, 1478 Lørenskog, Norway. Phone: +47-679-60000; Fax: +47-679-68861; E-mail: a.h.ree@medisin.uio.no

**Disclosure of Potential Conflicts of Interest:** The authors declare no potential conflicts of interest.

**Abstract**

Most patients with spread of large bowel cancer to other organs do not respond to immune therapy. We identified a rare gene mutation, termed 9p24.1 copy-number gain, in this otherwise incurable tumor that provoked an immune therapy response. We identified the chromosome 9p24.1 copy-number gain in a liver metastasis biopsy from a patient that had refractory disease to standard therapies, by gene-panel sequencing of DNA. Following immune checkpoint blockade with pembrolizumab (anti–PD-1), the patient experienced conversion of the tumor phenotype from one with epithelial features to that of an inflamed microenvironment, demonstrated by high-resolution RNA sequencing. Circulating tumor DNA disappeared over the first two weeks of therapy. As assessed by standard radiographic measurement, the patient had a partial response that was durable. This patient's response may support the use of histology-agnostic immune checkpoint blockade in solid tumors that carry the rare 9p24.1 copy-number gain.

## Introduction

The immune context of the tumor microenvironment (TME) determines the response to immune checkpoint blockade (ICB) in colorectal cancer (CRC; 1, 2). Favorable survival following ICB in metastatic disease from the minority of cases with primary CRC deficient in the DNA-mismatch repair (MMR) function is reflected by either high tumor mutational burden or positive microsatellite-instability (MSI) status (3, 4). Unlike for non-small-cell lung cancer (NSCLC), tumor-cell expression of the ligand of the programmed death receptor (PD-1), PD-L1, has not been used as a predictive biomarker of ICB response in CRC.

Despite the extensive immune-cell infiltrate recruited by the malignant Reed-Sternberg cells in classic Hodgkin's lymphoma, the cytotoxic immune cells are anergic. This is frequently caused by Reed-Sternberg-cell copy-number gain (CNG) of chromosome 9p24.1, which includes loci for *CD274*, *PDCD1LG2*, and *JAK2*. This CNG leads to enhanced expression of PD-L1, the PD-1 ligand PD-L2, and Janus kinase-2 (JAK2) and thereby maintains Reed-Sternberg-cell survival signaling, unless the evasion of T-cell cytotoxicity is revoked by ICB (5-8). CNG of the 9p24.1 locus, associated with susceptibility to ICB, has been observed in rare lymphoma entities, and its prevalence in solid tumors is low, estimated to only 0.2% of CRC cases (9).

The 'Actionable Targets in Cancer Metastasis' (MetAction) study (ClinicalTrials NCT02142036) established expedited and safe mutation profiling of an individual patients' progressing metastatic cancer following failure of systemic therapies, in order to offer histology-agnostic, molecularly matched medication for end-stage cancer (10). The treatment-refractory 9p24.1-CNG colon cancer case reported here illustrates the utility of this pipeline and further delineates the ICB response by diverse modalities.

## Materials and Methods

### Study procedures

The study was approved by the Institutional Review Board, the Regional Committee for Medical and Health Research Ethics of South-East Norway (reference number, REK 2013/2099), and the Norwegian Medicines Agency. It was performed in accordance with the Declaration of Helsinki. Written informed consent was required for participation. The study procedures and endpoints have been described previously (10) and are, together with details about the gene mutation profiling, provided in Supplementary Methods (10-12).

DNA/RNA extracted from biopsy-sampled metastatic tissue and from a whole blood sample as germline control at enrollment was sequenced using the Ion Oncomine™ Comprehensive Assay v1 (Thermo Fisher Scientific). The median sequencing depth was ~3000×, enabling calculation of the approximate mutant-allele fraction in heterogeneous tissue samples. The DNA sequence data was analyzed by the Torrent Suite™ software (Thermo Fisher Scientific); specifically, copy-number variants were detected in the copy-number detection module of the Ion Reporter™ software (Thermo Fisher Scientific). The called gene variants were filtered prior to assessment and prioritization. The Molecular Tumor Board interpreted the findings with regard to the likelihood of involved tumor signaling activity, delivering conclusions that the following Clinical Tumor Board used to recommend potential systemic tumor-directed medication.

Fluorescence *in-situ* hybridization analysis of the resected primary and locally recurrent tumors was performed to assess chromosome 9p copy-number, using a commercial probe pair that included a 350-kilobase 9p21.3-specific probe covering *CDKN2A* and *CDKN2B*, labeled with Platinum*Bright*™550, and a 440-kilobase 9q21-specific probe spanning from RH40366 to SHGC-82248, labeled with Platinum*Bright*™495 (both Kreatech™ probes KBI-10402).

Cell-free DNA was extracted from plasma sampled at each CT examination. The quantitative digital PCR assay, capable of discriminating between the *KRAS* p.G12D and wildtype sequences, was performed on the Raindrop™ system (RainDance™ Technologies).

RNA was extracted from liver metastasis biopsies sampled at study enrolment and 2 weeks of treatment for high-resolution sequence analysis that yielded a minimum of ~35 million reads per sample. Each transcript was quantified and compared for expression level in the two biopsy specimens. Differentially expressed genes were analyzed for significant biological functions and signaling pathways inherent in the tumor phenotype responses using the Ingenuity® Pathway Analysis software. Details on these procedures are provided in Supplementary Methods.

**Study treatment**

Following conclusion of the diagnostic procedure, the patient had a baseline computed tomography (CT) examination and commenced treatment with pembrolizumab (2 mg/kg every 3 weeks). Evaluation CT examinations were undertaken every 9 weeks. Routine blood tests were done within the standard patient work-up.

## Results

**Case history**

In October 2015, a 51-year-old woman with an otherwise unremarkable medical background presented with anemia and was diagnosed with a conventional-type colon adenocarcinoma located in the hepatic flexure and extending into the right liver lobe. The tumor was positive for the *KRAS* p.G12D mutation and MSI markers and devoid of the MMR protein PMS2. The patient was referred to neoadjuvant oxaliplatin-based chemotherapy [the

Nordic FLOX regimen (13)], but CT evaluation after 3 cycles revealed locally progressive disease. The patient underwent a right-sided hemicolectomy and in-continuity resection of the involved liver segments. Histological examination of the surgical specimen confirmed margin-negative ypT4bN0V0-stage disease. The patient was not offered adjuvant oncologic therapy.

Repeat CT scanning 4 months after the surgical procedure showed a locally recurrent tumor comprising the duodenum and pancreas, and the patient proceeded directly to salvage surgery. The histological examination noted a positive margin towards the posterior abdominal wall and tumor infiltration in a portal vein. One month post-operatively the patient commenced a 5-week-long chemoradiotherapy regimen (delivered to the involved area of dissection).

A repeat CT record 3 months after completion of the adjuvant treatment revealed one metastatic lesion in each liver lobe in addition to an enlarged portal hilum lymph node. The patient was assessed for palliative irinotecan-based chemotherapy [the Nordic FLIRI regimen (14)], but disease progression was noted after 4 cycles. Immune checkpoint inhibitors are not approved by Norwegian health authorities for treatment of advanced MSI-positive CRC within the public health services, thus, the patient was ineligible in routine clinical practice. In February 2017, she was enrolled in the MetAction study.

**Metastasis genome profiling**

Following study enrollment, ultrasound-guided core biopsies were taken from the metastatic lesion in the left liver lobe without procedure-induced complications. Tumor-cell content was 30% as assessed by tissue imprint. The DNA sequencing revealed point mutations commonly observed in CRC (*APC* p.R216X, *KRAS* p.G12D, and *FBXW7* p.R465H), each with approximately 30% mutant-allele fraction, in addition to an estimated

≥4-fold relative 9p-CNG (Fig. 1A), confirmed by fluorescence *in-situ* hybridization (Fig. 1B). Acknowledging the approximations by applying the Oncomine™ Comprehensive Assay to estimate the tumor mutational burden, defined as the number per megabase of coding synonymous base substitutions and indel mutations, but excluding known driver mutations (15), only one of the identified mutations was eligible. This corresponded to a tumor mutational burden rate of 5, which is typical for MMR-proficient CRC (16).

**Clinical response**

Following tumor board consensus supporting treatment with a PD-1 inhibitor and patient's commencement of pembrolizumab treatment, blood tests showed decline in tumor markers already at 2-3 weeks (Fig. 2A). The moderately elevated liver enzymes decreased over the entire treatment course; liver function markers as well as differential blood counts, electrolytes, and other renal function markers have all been within reference limits throughout therapy. The first CT evaluation after 3 treatment cycles revealed a partial response, according to the Response Evaluation Criteria in Solid Tumors v1.1, which remained consolidated at the 1-year treatment evaluation (Fig. 2B). The patient has been continuing the treatment for 20 months with ongoing partial response (by November 2018).

As shown by Supplementary Fig. S1, the patient experienced a rise in plasma free-$T_4$ and a corresponding fall in thyroid-stimulating hormone only 2-3 weeks after commencement of therapy. Grade 1 hyperthyroidism (by Common Terminology Criteria for Adverse Events v4.0) was evident when the patient started the third treatment cycle, whereas grade 2 hypothyroidism was recorded at commencement of cycle 4. Since then, the patient has been on continuous medication with levothyroxine that has been dose-adjusted based on the continuous monitoring of plasma thyroid-stimulating hormone and free-$T_4$. The patient has not reported other adverse events.

**Circulating tumor DNA (ctDNA) response**

Plasma analysis showed a decline in the *KRAS* mutant-allele fraction from 23% at baseline to 2.4% at 2 weeks of study treatment (Fig. 2C). A mutant-allele fraction of only 0.1% was detected in the concurrent liver metastasis biopsy. Plasma specimens sampled at each of the CT evaluations were negative for *KRAS* p.G12D (Fig. 2C).

**Metastasis phenotype response**

The RNA transcript profile of the left liver lobe metastasis (the individual RNA sequence counts are provided in Supplementary Table S1) changed over the first 2 weeks of PD-1 blockade (Supplementary Table S2). Although expression of *CD274* (PD-L1) and *JAK2* diminished, *PDCD1LG2* (PD-L2) expression increased in the on-treatment biopsy (Supplementary Table S3). Among the most discriminating RNA profile-defined functions altered between the baseline and 2-week samples were activation of responses ascribed to immune-cell trafficking, lipid metabolism, and inflammation, whereas biological features related to epithelial neoplasia were inhibited (Fig. 3A and Supplementary Table S4). Moreover, profile-defined signaling pathways that were induced by pembrolizumab included activation of the liver-X/retinoid-X hormone receptor transcription factors (LXR/RXR) and acute-phase reaction with the complement system (Fig. 3B and Supplementary Table S5). An 18-gene T-cell-inflamed expression profile that predicted response to pembrolizumab across multiple solid tumors has been reported (17). In our dataset, a majority of these interferon-γ-responsive genes were activated in the metastasis at 2 weeks of pembrolizumab treatment, whereas *IDO1* expression was repressed (Fig. 3C).

## Discussion

We report a radiographically partial and durable response of advanced colon cancer on PD-1 blockade based on 9p24.1-CNG detected in a metastatic liver lesion. A decline in circulating routine tumor markers and the mutant *KRAS* DNA was observed already following the first therapy cycle, mirroring the conversion of the metastasis phenotype from epithelial features to characteristics of an inflamed TME. The response measured with each of diverse modalities was consistent with the MetAction diagnostic procedure concluding that the CNG of chromosome 9p24.1 represented the driver alteration. This cause of ICB susceptibility is rare in solid tumors and particularly in CRC (9). One other case of advanced 9p24.1-CNG colon adenocarcinoma treated with a PD-1 inhibitor has been reported (18).

The therapeutic response came with a common toxicity, a transient hyperthyroidism preceding hypothyroidism that was managed by hormone substitution. Patients with advanced NSCLC have better response and outcome measures to ICB if they developed thyroid dysfunction, which was an independent predictive factor (19, 20). This suggests a mechanistic connection between the thyroid hormone metabolism and ICB efficacy. In mice, the $T_4$ metabolite triiodothyronine stimulated tumor-antigen-presenting dendritic cells to impel interferon-γ-mediated T-cell cytotoxicity (21).

Some studies have reported on the analysis of ctDNA to assess ICB efficacy in advanced cancer. A prospective pilot study of 10 patients with detectable ctDNA at commencement of therapy, including one MSI-positive CRC case, showed that complete ctDNA loss at the first treatment assessment (8 weeks) was associated with durable radiographic tumor response as well as long survival outcomes (22). An association between ctDNA and radiographic outcomes was also reported in 24 NSCLC cases (23). Our case showed 30% *KRAS* mutant-allele fraction in the baseline metastasis and only 0.1% at 2 weeks of treatment. The corresponding figures for ctDNA, 23% *versus* 2.4%, may reflect different

methodological sensitivity or tumor load at other metastatic sites. Nevertheless, plasma *KRAS* p.G12D was undetectable from the first radiographic response evaluation at 9 weeks onwards.

The conversion of the liver metastasis phenotype following initiation of the PD-1 inhibitor, as portrayed by the RNA sequence data, was perhaps the most intriguing observation. The interrelated phenotypes comprising *CD274* (PD-L1) and *JAK2* expression and sequences ascribed to intestinal epithelial neoplasia were attenuated, consistent with a rapid and substantial tumor-cell elimination. In contrast, expression of the chromosome 9p24.1 partner *PDCD1LG2* (PD-L2) was augmented in the 2-week biopsy sample. It has been proposed that PD-L2 positivity of tumor cells and TME cells predicts treatment response to PD-1 blockade through T-cell reactivity (24, 25). Hence, the heightened PD-L2 expression in the on-treatment metastasis specimen might have reflected activation of tumor-targeting immunity.

The computational RNA sequence analysis further revealed enrichment of pembrolizumab-induced functions and signaling pathways with designations such as immune-cell trafficking but also inflammation, acute-phase response, and complement system activity. The complement complex belongs to the rapidly responding innate immunity and exerts opposing effects within tumor-antigen presentation and T-cell-mediated cytotoxicity on the one side and TME activation of tumor-supportive systemic inflammation on the other (26). However, the data also supported pembrolizumab-induced activity of interferon-γ-responsive genes involved in tumor-eliminating T-cell effects (17). The patient has had no clinical or biochemical evidence of systemic inflammation during the treatment course. Expression of the interferon-γ-responsive *IDO1*, encoding the essential indoleamine 2,3-dioxygenase-1 of various TME-cell types that participate in immune tolerance to tumor antigens (27), was repressed at 2 weeks of ICB. Noting the failure or termination of clinical trials adding an

indoleamine 2,3-dioxygenase-1 inhibitor to PD-1 blockade, it may be that this particular combination is mechanistically redundant.

The RNA transcript profile also revealed a possible role of lipid metabolism and particularly LXR/RXR activity in the patient's metastatic cancer on ICB response. In mouse models, administration of an LXR agonist reduced the numbers of systemic and tumor-infiltrating myeloid-derived suppressor-cells (an innate immune-cell population), which evoked T-cell cytotoxicity and restrained tumor growth; similar effects on peripheral blood myeloid-derived suppressor-cells and cytotoxic T-cells were observed in patients (28). It has been known for almost three decades that LXR/RXR function as co-regulators of thyroid hormone receptor-mediated transcription (29). However, in our patient's case, it is not clear how the initial hyperthyroidism and the concurrent ICB-induced LXR/RXR activity in the metastatic cancer were mechanistically interrelated.

The patient described here, presenting to the MetAction study with metastatic colon cancer refractory to all standard therapies, has experienced durable, near-complete radiographic tumor regression following administration of pembrolizumab based on the detection of 9p24.1-CNG in a liver metastasis. Our experience may support the use of PD-1 blockade in histology-agnostic cases with 9p24.1-CNG.

## Data Sharing

Request to inspect and analyze the data that underlie the results reported in this article, including the sequence datasets that are stored in the Services for Sensitive Data facility at University of Oslo, should be directed to the corresponding author, and access will be provided in accordance with the General Data Protection Regulation of the European Union.


## Acknowledgments

This work was supported by grants from the Research Council of Norway (218325) and South-Eastern Norway Regional Health Authority (2017109). We thank the Norwegian Cancer Genome Consortium for the opportunity to use their resources in the analysis and handling of DNA/RNA sequence data. The esthetic creation of the figure artwork by Ms. Dawn Patrick-Brown is highly appreciated.

**References**

1. Dienstmann R, Vermeulen L, Guinney J, Kopetz S, Tejpar S, Tabernero J. Consensus molecular subtypes and the evolution of precision medicine in colorectal cancer. Nat Rev Cancer 2017;17:79–92.

2. Grasso CS, Giannakis M, Wells DK, Hamada T, Mu XJ, Quist M, et al. Genetic mechanisms of immune evasion in colorectal cancer. Cancer Discov 2018;8:730–49.

3. Le DT, Uram JN, Wang H, Bartlett BR, Kemberling H, Eyring AD, et al. PD-1 blockade in tumors with mismatch-repair deficiency. N Engl J Med 2015;372:2509–20.

4. Le DT, Durham JN, Smith KN, Wang H, Bartlett BR, Aulakh LK, et al. Mismatch repair deficiency predicts response of solid tumors to PD-1 blockade. Science 2017;357:409–13.

5. Ansell SM, Lesokhin AM, Borrello I, Halwani A, Scott EC, Gutierrez M, et al. PD-1 blockade with nivolumab in relapsed or refractory Hodgkin's lymphoma. N Engl J Med 2015;372:311–9.

6. Armand P, Shipp MA, Ribrag V, Michot JM, Zinzani PL, Kuruvilla J, et al. Programmed death-1 blockade with pembrolizumab in patients with classic Hodgkin lymphoma after brentuximab vedotin failure. J Clin Oncol 2016;34:3733–9.

7. Chen R, Zinzani PL, Fanale MA, Armand P, Johnson NA, Brice P, et al. Phase II study of the efficacy and safety of pembrolizumab for relapsed/refractory classic Hodgkin lymphoma. J Clin Oncol 2017;35:2125–32.

8. Younes A, Santoro A, Shipp M, Zinzani PL, Timmerman JM, Ansell S, et al. Nivolumab for classical Hodgkin's lymphoma after failure of both autologous stem-cell transplantation and brentuximab vedotin: a multicentre, multicohort, single-arm phase 2 trial. Lancet Oncol 2016;17:1283–94.

9. Goodman AM, Piccioni D, Kato S, Biochard A, Wang HY, Frampton G, et al. Prevalence of PDL1 amplification and preliminary response to immune checkpoint blockade in solid tumors. JAMA Oncol 2018;4:1237–44.

10. Ree AH, Russnes HG, Heinrich D, Dueland S, Boye K, Nygaard V, et al. Implementing precision cancer medicine in the public health services of Norway: the diagnostic infrastructure and a cost estimate. ESMO Open 2017;2:e000158.

11. Robinson JT, Thorvaldsdóttir H, Winckler W, Guttman M, Lander ES, Getz G, et al. Integrative Genomics Viewer. Nat Biotechnol 2011;29:24–6.

12. Yang H, Wang K. Genomic variant annotation and prioritization with ANNOVAR and wANNOVAR. Nat Protoc 2015;10:1556–66.

13. Tveit KM, Guren T, Glimelius B, Pfeiffer P, Sorbye H, Pyrhonen S, et al. Phase III trial of cetuximab with continuous or intermittent fluorouracil, leucovorin, and oxaliplatin (Nordic FLOX) versus FLOX alone in first-line treatment of metastatic colorectal cancer: the NORDIC-VII study. J Clin Oncol 2012;30:1755–62.

14. Glimelius B, Sørbye H, Balteskard L, Byström P, Pfeiffer P, Tveit K, et al. A randomized phase III multicenter trial comparing irinotecan in combination with the Nordic bolus 5-FU and folinic acid schedule or the bolus/infused de Gramont schedule (Lv5FU2) in patients with metastatic colorectal cancer. Ann Oncol 2008;19:909–14.

15. Chalmers ZR, Connelly CF, Fabrizio D, Gay L, Ali SM, Ennis R, et al. Analysis of 100,000 human cancer genomes reveals the landscape of tumor mutational burden. Genome Med 2017;9:34.

16. Yarchoan M, Hopkins A, Jaffee EM. Tumor mutational burden and response rate to PD-1 inhibition. N Engl J Med 2017;377:2500–1.

17. Ayers M, Lunceford J, Nebozhyn M, Murphy E, Lobonda A, Kaufman DR, et al. IFN-γ-related mRNA profile predicts clinical response to PD-1 blockade. J Clin Invest 2017;127:2930–40.

18. Sorscher S, Resnick J, Goodman M. First case report of a dramatic radiographic response to a checkpoint inhibitor in a patient with proficient mismatch repair gene expressing metastatic colorectal cancer. JCO Precis Oncol 2017.

19. Osorio JC, Ni A, Chaft JE, Pollina R, Kasler MK, Stephens D, et al. Antibody-mediated thyroid dysfunction during T-cell checkpoint blockade in patients with non-small-cell lung cancer. Ann Oncol 2017;28:583–9.

20. Kim HI, Kim M, Lee SH, Park SY, Kim YN, Kim H, et al. Development of thyroid dysfunction is associated with clinical response to PD-1 blockade treatment in patients with advanced non-small cell lung cancer. Oncoimmunology 2017;7:e1375642.

21. Alamino VA, Mascanfroni ID, Montesinos MM, Gigena N, Donadio AC, Blidner AG, et al. Antitumor responses stimulated by dendritic cells are improved by triiodothyronine binding to the thyroid hormone receptor β. Cancer Res 2015;75:1265–74.

22. Cabel L, Riva F, Servois V, Livartowski A, Daniel C, Rampanou A, et al. Circulating tumor DNA changes for early monitoring of anti-PD1 immunotherapy: a proof-of-concept study. Ann Oncol 2017;28:1996–2001.

23. Goldberg SB, Narayan A, Kole AJ, Decker RH, Teysir J, Carriero NJ, et al. Early assessment of lung cancer immunotherapy response via circulating tumor DNA. Clin Cancer Res 2018;24:1872–80.

24. Yearley JH, Gibson C, Yu N, Moon C, Murphy E, Juco J, et al. PD-L2 expression in human tumors: relevance to anti-PD-1 therapy in cancer. Clin Cancer Res 2017;23:3158–67.

25. Ahmad SM, Martinenaite E, Holmström M, Jørgensen MA, Met Ö, Nastasi C, et al. The inhibitory checkpoint, PD-L2, is a target for effector T cells: novel possibilities for immune therapy. Oncoimmunology 2017;7:e1390641.

26. Reis ES, Mastellos DC, Ricklin D, Mantovani A, Lambris JD. Complement in cancer: untangling an intricate relationship. Nat Rev Immunol 2018;18:5–18.

27. Prendergast GC, Malachowski WP, DuHadaway JB, Muller AJ. Discovery of IDO1 inhibitors: from bench to bedside. Cancer Res 2017;77:6795–811.

28. Tavazoie MF, Pollack I, Tanqueco R, Ostendorf BN, Reis BS, Gonsalves FC, et al. LXR/ApoE activation restricts innate immune suppression in cancer. Cell 2018;172:825–40.

29. Yu VC, Delsert C, Andersen B, Holloway JM, Devary OV, Näär AM, et al. RXRβ: a coregulatory that enhances binding of retinoic acid, thyroid hormone, and vitamin D receptors to their cognate response elements. Cell 1991;67:1251–66.

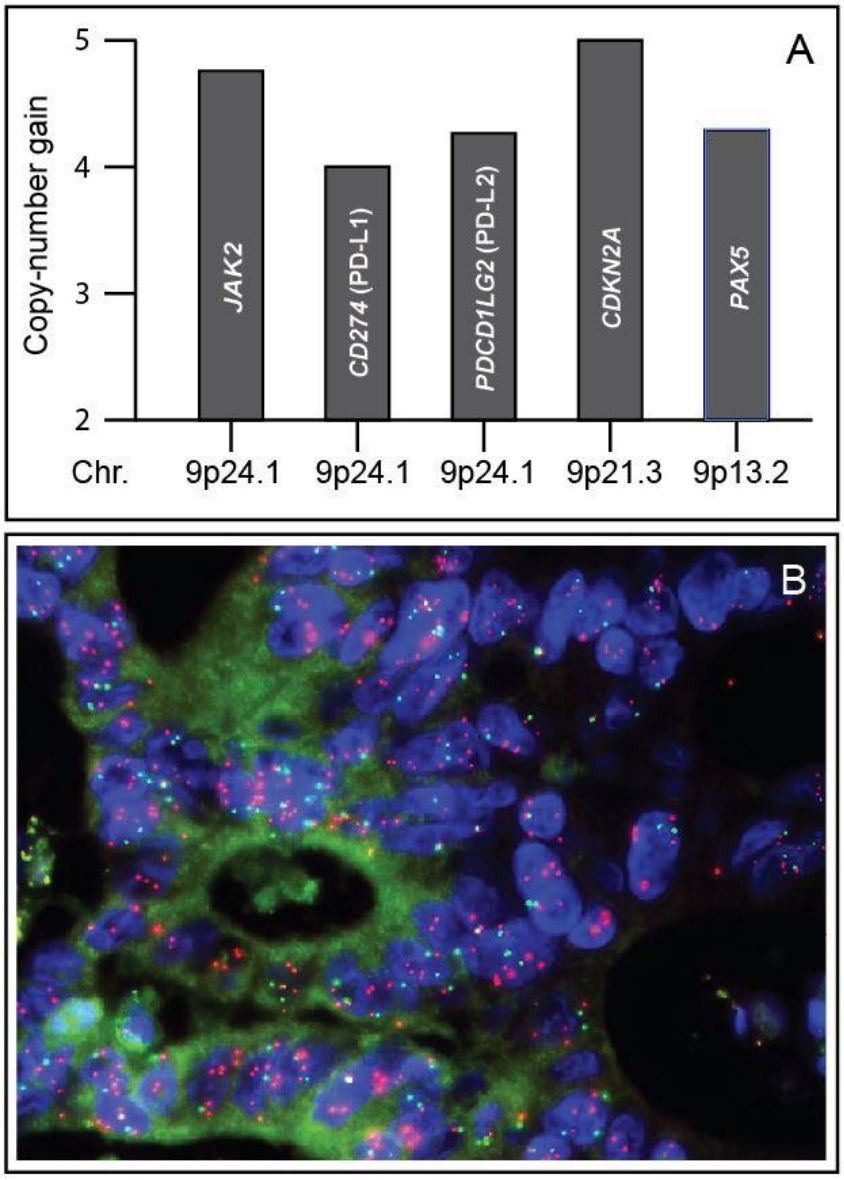


**Figure 1.**

Chromosome (Chr.) 9p copy-number gain. Panel **A** shows the genes within the 9p amplicon, as covered by the Oncomine™ Comprehensive Assay and each with its relative copy-number gain, identified in the liver metastasis specimen sampled at study enrolment. Panel **B** shows nuclei from the primary tumor specimen with 9p21.3 copy-number gain [9p21.3 (red signals) to 9q21 (green signals) ratio of 3.4 from the average copy numbers of 4.7 for 9p21.3 and 1.4 for 9q21], as assessed by fluorescence *in-situ* hybridization.

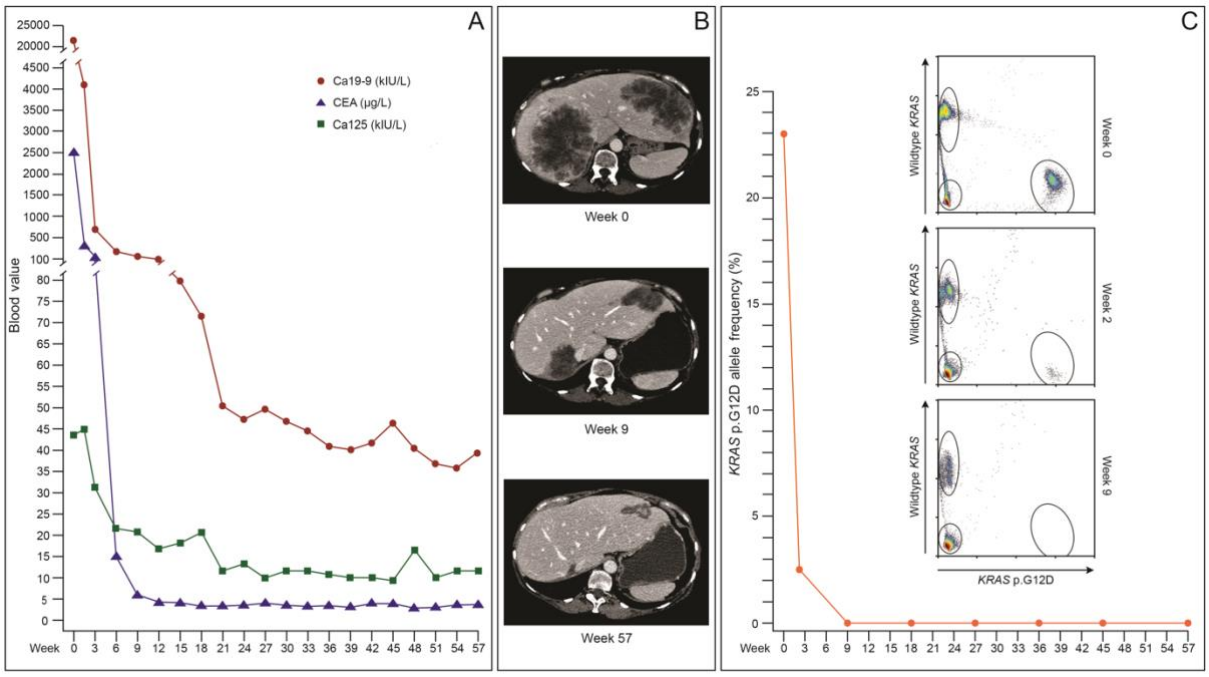


**Figure 2.**

Tumor response to the study treatment. Panel **A** shows amounts of circulating tumor markers over the treatment course. The start of a new treatment cycle corresponds to the given week numbers. Panel **B** shows one transverse-view image from each of portovenous-phase contrast-enhanced computed tomographic scans of the abdomen recorded before commencement of the study treatment (top panel), at the first evaluation (middle panel), and at the 1-year evaluation (bottom panel). Longest cross-sectional perpendicular measures at these points were for the right liver lobe lesion: 120 mm × 100 mm, 56 mm × 46 mm, and 25 mm × 15 mm; for the left liver lobe lesion: 125 mm × 66 mm, 79 mm × 37 mm, and 52 mm × 22 mm; for the short axis of the portal hilum lymph node (not depicted on the selected images): 26 mm, 22 mm, and 13 mm. Panel **C** shows the circulating amounts of the mutant KRAS relative to the wildtype variant over the treatment course. The inserted histograms show the quantification by digital PCR of the two *KRAS* alleles before the start (top panel) and at 2 weeks (middle panel) and 9 weeks (bottom panel) of the study treatment.

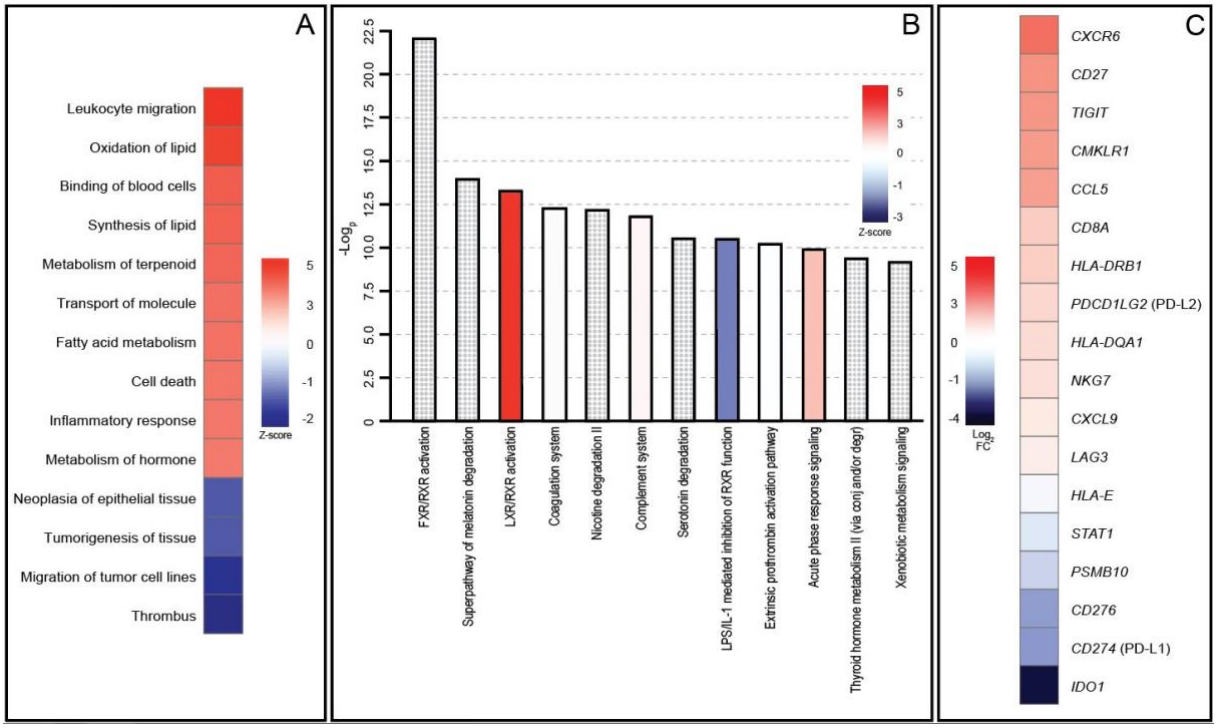


**Figure 3.**

Phenotypic response to the immune checkpoint blockade. Panel **A** shows annotated functions, as defined by the Ingenuity® Pathway Analysis software, based on differentially expressed genes ($n$ = 4,168) in the 2-week *versus* baseline biopsy specimen from the left liver lobe metastasis, ranked by z-score. The resulting functions (Supplementary Table S4) were filtered according to the following criteria: z-score higher than 3.4 or lower than –1.6, $p < 3\times10^{-6}$, and removal of redundant functions. Panel **B** shows the software's signaling pathway annotation of the input genes, ranked by $p$-value and following removal of redundant pathways (from Supplementary Table S5); patterned bars, no z-score. Panel **C** shows $\log_2$ fold-change (FC) expression of 18 interferon-γ-responsive genes, which define a profile predictive of response to immune checkpoint blockade (17), in the 2-week *versus* baseline biopsy specimen.